J. Fluid Mech. (1992), *vol.* 237, *pp.* 323–341
Printed in Great Britain

Flow past a sphere with an oscillation in the free-stream velocity and unsteady drag at finite Reynolds number

By RENWEI MEI† AND RONALD J. ADRIAN
Department of Theoretical and Applied Mechanics, University of Illinois, Urbana, IL 61801, USA

(Received 15 January 1991 and in revised form 30 September 1991)

Unsteady flow over a stationary sphere with a small fluctuation in the free-stream velocity is considered at small Reynolds number, Re. A matched asymptotic solution is obtained for the frequency-dependent (or the acceleration-dependent) part of the unsteady flow at very small frequency, ω, under the restriction $St \ll Re \ll 1$, where St is the Strouhal number. The acceleration-dependent part of the unsteady drag is found to be proportional to $St \sim \omega$ instead of the $\omega^{\frac{1}{2}}$ dependence predicted by Stokes' solution. Consequently, the expression for the Basset history force is incorrect for large time even for very small Reynolds numbers. Present results compare well with the previous numerical results of Mei, Lawrence & Adrian (1991) using a finite-difference method for the same unsteady flow at small Reynolds number. Using the principle of causality, the present analytical results at small Re, the numerical results at finite Re for low frequency, and Stokes' results for high frequency, a modified expression for the history force is proposed in the time domain. It is confirmed by comparing with the finite-difference results at arbitrary frequency through Fourier transformation. The modified history force has an integration kernel that decays as t^{-2}, instead of $t^{-\frac{1}{2}}$, at large time for both small and finite Reynolds numbers.

1. Introduction

In a recent paper (Mei, Lawrence & Adrian 1991, hereinafter referred as MLA), numerical results are obtained for the unsteady drag on a sphere at finite Reynolds number with a small oscillation in the free-stream velocity in the form of $U_\infty(t) = U(1+\alpha_1 e^{-i\omega t'})$ with $\alpha_1 \ll 1$, U being the mean free-stream velocity, ω the frequency of the oscillation, t' the dimensional time. The calculations are based on the finite-difference method of Mei & Plotkin (1986) using the stream function–vorticity formulation. It is found that the classical Stokes solution of the unsteady Stokes equation does not correctly describe the behaviour of the unsteady drag at low frequency. The numerical results indicate that the force increases linearly with frequency when the frequency is very small instead of the square root of the frequency as the classical Stokes solution predicts. This implies that in the time domain the Basset force (Basset 1888) has a much shorter memory than that predicted by classical theory.

To gain insight into the unsteady particle dynamics, especially at low frequency,

† Present address: Department of Aerospace Engineering, Mechanics & Engineering Science, University of Florida, Gainesville, FL 32611, USA.

and to obtain a more realistic expression of the history force, we reconsider the same unsteady flow problem discussed in MLA using analytical approaches.

Following Lighthill (1954), a regular perturbation scheme is applied first to decompose the solution into a steady part and an unsteady part by assuming a small amplitude of the oscillation in the free stream velocity. The method of matched asymptotic expansion is used to solve for the unsteady flow field at low Reynolds number and small frequency. The solution for the unsteady part is analogous to that of Proudman & Pearson (1957) for the steady part. For small Strouhal number, St (or low frequency) two terms of the unsteady solution are sought. The first corresponds to the quasi-steady state; its outer solution can be obtained easily by differentiating the steady outer solution of Proudman & Pearson (1957). The second term is acceleration dependent. Its solution is obtained separately in the inner region and the outer region. The acceleration-dependent drag is found to be linearly proportional to the Strouhal number, St. The analytical value of the drag coefficient at small Re and St agrees well with the value computed using the finite-difference method.

After the drag at low frequency ($St \ll Re$) is determined, it is used along with the Stokes solution at high frequency and the numerical results at finite Re to construct an expression for the unsteady drag. The integration kernal for the history force is determined based on the principle of causality. The new history force, which decays as t^{-2} at large time, has a much shorter memory than that predicted by the classical Basset solution.

2. Asymptotic expansion of the unsteady Navier–Stokes equation at $St \ll Re \ll 1$

2.1. *Governing equation and the steady-state solution*

As has been discussed in MLA, the unsteady Stokes equation is not adequate to describe the flow field at small Strouhal number, St, because the nonlinear convection term that is neglected in the Stokes equation may be larger than the unsteady term in the complete Navier–Stokes equation.

In terms of the stream function in the spherical coordinates (r, θ, ϕ), the complete, unsteady, dimensionless Navier–Stokes equation for axisymmetric flow is

$$St\,Re'\frac{\partial}{\partial t}(\mathrm{D}_r^2\psi)+Re'\left[\frac{1}{r^2}\frac{\partial(\psi,\mathrm{D}_r^2\psi)}{\partial(r,\mu)}+\frac{2}{r^2}\mathrm{D}_r^2\psi\,\mathrm{L}_r\psi\right]=\mathrm{D}_r^4\psi. \tag{1}$$

In the above,

$$\left.\begin{aligned}&\mu=\cos\theta,\\ &\mathrm{D}_r^2=\frac{\partial^2}{\partial r^2}+\frac{1-\mu^2}{r^2}\frac{\partial^2}{\partial\mu^2},\quad \mathrm{L}_r=\frac{\mu}{1-\mu^2}\frac{\partial}{\partial r}+\frac{1}{r}\frac{\partial}{\partial\mu},\\ &\frac{\partial(A,B)}{\partial(r,\mu)}=\frac{\partial A}{\partial r}\frac{\partial B}{\partial\mu}-\frac{\partial A}{\partial\mu}\frac{\partial B}{\partial r},\end{aligned}\right\} \tag{2}$$

and

$$\left.\begin{aligned}Re' &= Ua/\nu = \text{Reynolds number based on radius of the sphere,}\\ St &= \omega a/U = \text{Strouhal number.}\end{aligned}\right\} \tag{3}$$

Here, a is the radius of the sphere and ν is the kinematic viscosity of the fluid. The stream function in (1) and the operator D_r^2 have been scaled by Ua^2 and $1a^2$

respectively. (Note that $Re = U2a/\nu = 2Re'$ was used in MLA.) The boundary conditions for oscillating axisymmetric flow are

$$\psi = \frac{\partial\psi}{\partial r} = \frac{\partial\psi}{\partial\mu} = 0 \qquad \text{on} \quad r = 1, \tag{4}$$

$$\psi \to \tfrac{1}{2}(1+\alpha_1 \mathrm{e}^{-\mathrm{i}t})\, r^2(1-\mu^2) \quad \text{as} \quad r \to \infty. \tag{5}$$

To solve (1), a regular perturbation scheme for the flow field is applied first. This technique is the same as in the numerical work of MLA. It was used by Lighthill (1954) and Ackerberg & Phillips (1972) to study unsteady boundary layers with small fluctuations in the magnitude of the free-stream velocity. Let

$$\psi(r,\mu,t) = \psi_{\mathrm{s}}(r,\mu) + \alpha_1 \mathrm{e}^{-\mathrm{i}t}\psi_1(r,\mu) + O(\alpha_1^2), \tag{6}$$

where ψ_{s} and $\alpha_1\psi_1$ correspond to the steady-state solution and the amplitude of the first-harmonic unsteady flow. Substituting (6) into (1) and collecting the terms of $O(1)$ and $O(\alpha_1)$, one has

$$Re'\left[\frac{1}{r^2}\frac{\partial(\psi_{\mathrm{s}}, \mathrm{D}_r^2\psi_{\mathrm{s}})}{\partial(r,\mu)} + \frac{2}{r^2}\mathrm{D}_r^2\psi_{\mathrm{s}}\,\mathrm{L}_r\psi_{\mathrm{s}}\right] = \mathrm{D}_r^4\psi_{\mathrm{s}} \tag{7}$$

and

$$-\mathrm{i}\,St\,Re'\,\mathrm{D}_r^2\psi_1 + Re'\left[\frac{1}{r^2}\frac{\partial(\psi_{\mathrm{s}}, \mathrm{D}_r^2\psi_1)}{\partial(r,\mu)} + \frac{1}{r^2}\frac{\partial(\psi_1, \mathrm{D}_r^2\psi_{\mathrm{s}})}{\partial(r,\mu)} + \frac{2}{r^2}(\mathrm{D}_r^2\psi_{\mathrm{s}}\,\mathrm{L}_r\psi_1 + \mathrm{D}_r^2\psi_1 L_r\psi_{\mathrm{s}})\right] = \mathrm{D}_r^4\psi_1. \tag{8}$$

The boundary conditions for ψ_{s} and ψ_1 are identical:

$$\psi = \frac{\partial\psi}{\partial r} = \frac{\partial\psi}{\partial\mu} = 0 \qquad \text{on} \quad r = 1, \tag{9}$$

$$\psi \to \tfrac{1}{2}r^2(1-\mu^2) \qquad \text{as} \quad r \to \infty. \tag{10}$$

A solution to the steady-state equation (7) for $Re \ll 1$ has been given in Proudman & Pearson (1957). The inner solution for ψ_{s} is

$$\psi_{\mathrm{s}} = \frac{1}{4}\left(2r^2 - 3r + \frac{1}{r}\right)(1-\mu^2) + Re'\left[\frac{3}{32}\left(2r^2 - 3r + \frac{1}{r}\right)(1-\mu^2) + \frac{3}{16}\left(2r^2 - 3r + 1 - \frac{1}{r} + \frac{1}{r^2}\right)Q_2(\mu)\right] + \text{h.o.t.} = \psi_{\mathrm{s}0} + Re'\psi_{\mathrm{s}1} + \text{h.o.t.}, \tag{11}$$

where h.o.t. denotes higher-order terms. This is accurate up to $O(Re')$ and is valid for $r \approx O(1)$. The outer solution is

$$\begin{aligned}\Psi_{\mathrm{s}}(\rho,\mu) &= Re'^2\,\psi_{\mathrm{s}}(r,\mu) \\ &= \tfrac{1}{2}\rho^2(1-\mu^2) - Re'\,\tfrac{3}{2}Q_0(\mu)\,[1-\exp(-\tfrac{1}{2}\rho(1-\mu))] + \text{h.o.t.} \\ &= \Psi_{\mathrm{s}0} + Re'\,\Psi_{\mathrm{s}1} + \text{h.o.t.}\end{aligned} \tag{12}$$

In the above,

$$\rho = Re'\,r, \tag{13}$$

$$Q_n(\mu) \equiv \int_{-1}^{\mu} p_n(\mu)\,\mathrm{d}\mu, \tag{14}$$

with $p_n(\mu)$ being the Legendre polynomial of degree n. In particular, $Q_0(\mu) = 1+\mu$ and $Q_2(\mu) = -\frac{1}{2}\mu(1-\mu^2)$. The uniformly valid solution, which is accurate up to $O(Re')$, happens to be the Oseen's solution

$$\psi_s(r,\mu) \approx \tfrac{1}{2}r^2(1-\mu^2) - \frac{3}{2Re'}(1+\mu)\{1-\exp[-\tfrac{1}{2}Re'r(1-\mu)]\}. \tag{15}$$

Following Proudman & Pearson, we shall pursue approximate solutions to the unsteady equation (8) for the inner and outer regions separately.

2.2. *Inner and outer expansions for the unsteady solution*

In the inner (Stokes) region, the solution to (8) for $St \ll Re' \ll 1$ can be sought in the form

$$\psi_1 = [\psi_{10} + Re'\,\psi_{11} + \ldots] + St[\psi_{20} + Re'\,\psi_{21} + \ldots] + \ldots. \tag{16}$$

Substitution of (11) and (16) into (8) leads to

$O(1)$:
$$\mathrm{D}_r^4 \psi_{10} = 0, \tag{17}$$

$O(Re')$:
$$\mathrm{D}_r^4 \psi_{11} = \frac{1}{r^2}\frac{\partial(\psi_{s0}, \mathrm{D}_r^2\psi_{10})}{\partial(r,\mu)} + \frac{1}{r^2}\frac{\partial(\psi_{10}, \mathrm{D}_r^2\psi_{s0})}{\partial(r,\mu)} + \frac{2}{r^2}[\mathrm{D}_r^2\psi_{s0}\,\mathrm{L}_r\psi_{10} + D_r^2\psi_{10}\,\mathrm{L}_r\psi_{s0}], \tag{18}$$

$O(St)$:
$$\mathrm{D}_r^4 \psi_{20} = 0, \tag{19}$$

$O(St\,Re')$:
$$\mathrm{D}_r^4 \psi_{21} = \frac{1}{r^2}\frac{\partial(\psi_{s0}, \mathrm{D}_r^2\psi_{20})}{\partial(r,\mu)} + \frac{1}{r^2}\frac{\partial(\psi_{20}, \mathrm{D}_r^2\psi_{s0})}{\partial(r,\mu)} + \frac{2}{r^2}[\mathrm{D}_r^2\psi_{s0}\,\mathrm{L}_r\psi_{20} + \mathrm{D}_r^2\psi_{20}\,L_r\psi_{s0}] - \mathrm{i}\mathrm{D}_r^2\psi_{10}. \tag{20}$$

The boundary conditions for the inner solutions governed by (17)–(20) are

$$\psi_{nm} = \frac{\partial\psi_{nm}}{\partial r} = \frac{\partial\psi_{nm}}{\partial\mu} = 0 \quad \text{on} \quad r = 1 \tag{21}$$

for $nm = 1\,0,\ 1\,1,\ 2\,0$ and $2\,1$.

The equation for the stream function in the outer (Oseen's) region, with $\rho = Re'\,r \sim O(1)$, is

$$-\mathrm{i}\frac{St}{Re'}\mathrm{D}_\rho^2\Psi_1 + \frac{1}{\rho^2}\left[\frac{\partial(\Psi_s, \mathrm{D}_\rho^2\Psi_1)}{\partial(\rho,\mu)} + \frac{\partial(\Psi_1, \mathrm{D}_\rho^2\Psi_s)}{\partial(\rho,\mu)}\right] + \frac{2}{\rho^2}[\mathrm{D}_\rho^2\Psi_s\,\mathrm{L}_\rho\Psi_1 + \mathrm{D}_\rho^2\Psi_1\,\mathrm{L}_\rho\Psi_s] = \mathrm{D}_\rho^4\Psi_1, \tag{22}$$

where
$$\Psi_1 = Re'^2\psi_1. \tag{23}$$

In order to perform the asymptotic expansion for the small-frequency case, the unsteady term is assumed to be much smaller than the rest of the terms in both the inner and the outer regions. This requires $St/Re' \ll 1$ as (22) suggests. On the other hand, the inner solutions only require $St \ll 1$, which is less restrictive than the former, for (16) to hold. This suggests, formally, the use of St/Re' as a small parameter in the expansion of the outer solution.

The outer solution can thus be pursued formally in the form

$$\Psi_1 = [\Psi_{10} + Re'\,\Psi_{11} + \ldots] + \frac{St}{Re'}[\Psi_{20} + Re'\,\Psi_{21} + \ldots] + \ldots. \tag{24}$$

The boundary conditions for the outer solutions at infinity are

$$U_{11} \sim U_{20} \sim U_{21} \to 0 \quad \text{and} \quad \Psi_1 \to \tfrac{1}{2}\rho^2(1-\mu^2) \quad \text{as} \quad \rho \to \infty, \tag{25}$$

where U_{nm} represents the outer velocity of the corresponding order.

The solution to the first term, Ψ_{10}, is the uniform-stream solution satisfying the boundary condition as $\rho \to \infty$,

$$\Psi_{10} = \tfrac{1}{2}\rho^2(1-\mu^2). \tag{26}$$

The equations governing the remaining terms in (24) become

$$O(Re'): \quad \frac{(1-\mu^2)}{\rho}\frac{\partial \mathrm{D}_\rho^2 \Psi_{11}}{\partial \mu} + \mu\frac{\partial \mathrm{D}_\rho^2 \Psi_{11}}{\partial \rho} + \frac{1-\mu^2}{\rho}\frac{\partial \mathrm{D}_\rho^2 \Psi_{s1}}{\partial \mu} + \mu\frac{\partial \mathrm{D}_\rho^2 \Psi_{s1}}{\partial \rho} = \mathrm{D}_\rho^4 \Psi_{11}, \tag{27}$$

$$O\left(\frac{St}{Re'}\right): \quad \frac{(1-\mu^2)}{\rho}\frac{\partial \mathrm{D}_\rho^2 \Psi_{20}}{\partial \mu} + \mu\frac{\partial D_\rho^2 \Psi_{20}}{\partial \rho} = \mathrm{D}_\rho^4 \Psi_{20}, \tag{28}$$

$$O(St): \quad -\mathrm{i}\mathrm{D}_\rho^2 \Psi_{11} + \frac{(1-\mu^2)}{\rho}\frac{\partial \mathrm{D}_\rho^2 \Psi_{21}}{\partial \mu} + \mu\frac{\partial \mathrm{D}_\rho^2 \Psi_{21}}{\partial \rho} + \frac{1}{\rho^2}\left[\frac{\partial(\Psi_{s1}, \mathrm{D}_\rho^2 \Psi_{20})}{\partial(\rho,\mu)} + \frac{\partial(\Psi_{20}, \mathrm{D}_\rho^2 \Psi_{s1})}{\partial(\rho,\mu)}\right]$$
$$+ \frac{2}{\rho^2}[\mathrm{D}_\rho^2 \Psi_{20}\,\mathrm{L}_\rho \Psi_{s1} + \mathrm{D}_\rho^2 \Psi_{s1}\,\mathrm{L}_\rho \Psi_{20}] = \mathrm{D}_\rho^4 \Psi_{21}. \tag{29}$$

2.3. *Quasi-steady* ($St = 0$) *solutions in the inner and outer regions*

The solution for the quasi-steady state flow is sought first. Equation (17) is the classical Stokes equation. The general solution for ψ_{10}, which satisfies the boundary conditions at $r = 1$ and matches the outer solution given by (26) to $O(\rho^2)$, is

$$\psi_{10} = \tfrac{1}{4}(2r^2 - 3r + 1/r)(1-\mu^2). \tag{30}$$

The remaining terms in ψ_{10} are to be matched to higher-order outer solutions.

The outer solution for Ψ_{11} is obtained by taking the appropriate partial derivative of Ψ_{10} with respect to the fluctuating free-stream velocity, as suggested by Lighthill (1954), as

$$\Psi_{11} = -\tfrac{3}{4}\rho(1-\mu^2)\exp[-\tfrac{1}{2}\rho(1-\mu)]. \tag{31}$$

See also Mei (1990) for details. It can be shown to satisfy (27) by direct substitution.

As $\rho \to 0$, Ψ_{11} in (31) should match the rotational part of the inner (Stokes) solution ψ_{10} in (30). As $Re' \to 0$, the one-term expansion of the two-term outer solution written in the inner variable gives

$$\frac{1}{Re'^2}[\Psi_{10} + Re'\,\Psi_{11}] = \frac{1}{2}\frac{1}{Re'^2}\rho^2(1-\mu^2) - \frac{1}{Re'}\tfrac{3}{4}\rho(1-\mu^2)\,\mathrm{e}^{-\rho(1-\mu)/2}$$
$$\sim \tfrac{1}{2}r^2(1-\mu^2) - \tfrac{3}{4}r(1-\mu^2) + O(Re'). \tag{32}$$

This matches the first two terms of the one-term solution, ψ_{10}, given by (30). With the solutions for ψ_{10}, Ψ_{10} and Ψ_{11} obtained, the solution to (18) for ψ_{11} can now be sought.

Following Proudman & Pearson (1957), (18) becomes

$$\mathrm{D}_r^4 \psi_{11} = 9\left(\frac{2}{r^2} - \frac{3}{r^3} + \frac{1}{r^5}\right)Q_2(\mu). \tag{33}$$

A particular solution (33) that satisfies the boundary conditions at $r = 1$ and the symmetry conditions at $\mu = \pm 1$ is

$$\psi_{11}^{\mathrm{p}} = \frac{3}{8}\left(2r^2 - 3r + 1 - \frac{1}{r} + \frac{1}{r^2}\right) Q_2(\mu). \tag{34}$$

Rewriting (32) and keeping two terms of every order,

$$\frac{1}{Re'^2}[\Psi_{10} + Re'\,\Psi_{11}] \sim \tfrac{1}{2}r^2(1-\mu^2) - \tfrac{3}{4}r(1-\mu^2) + Re'[\tfrac{3}{8}r^2(1-\mu^2) + \tfrac{3}{4}r^2 Q_2(\mu)] + \text{h.o.t.} \tag{35}$$

To match the $O(Re')$ term in (35), the inner solution ψ_{11} must be, as a combination of general solution ψ_{11}^{g} and particular solution ψ_{11}^{p},

$$\begin{aligned}\psi_{11} &= \psi_{11}^{\mathrm{g}} + \psi_{11}^{\mathrm{p}} \\ &= \frac{3}{16}\left(2r^2 - 3r + \frac{1}{r}\right)(1-\mu^2) + \frac{3}{8}\left(2r^2 - 3r + 1 - \frac{1}{r} + \frac{1}{r^2}\right) Q_2(\mu).\end{aligned} \tag{36}$$

Obviously, the first two leading-order terms of (36) as $r \to \infty$ match the two $O(Re')$ terms in (35). The quasi-steady drag up to $O(Re')$ based on $(\psi_{10} + Re'\,\psi_{11})$ is thus

$$D_{\mathrm{QS}}/D_{\mathrm{S}} = \alpha_1 \mathrm{e}^{-\mathrm{i}t}(1 + \tfrac{3}{8}Re'), \tag{37}$$

where $D_{\mathrm{S}} = 6\pi\mu Ua$ is the Stokes drag. In deriving (37), it is noted that the second term in (36) does not contribute to the drag because of its antisymmetry. The first term in (36) is proportional to the Stokes solution for steady flow over a sphere with a proportionality constant of $\frac{3}{4}$. This observation will be used later in deriving (59).

2.4. *Acceleration-dependent solution in the inner and outer regions*

From (19), (20) and (28), (29), we see that the linear equations governing ψ_{20} and Ψ_{20} are homogeneous while those governing ψ_{21} and Ψ_{21} are driven by $\mathrm{D}_r^2\,\psi_{11}$ and $\mathrm{D}_\rho^2\,\Psi_{11}$. Starting from the outer solution, equation (28) for Ψ_{20} can be solved as follows. The general solution for $\mathrm{D}_\rho^2\,\Psi_{20}$ is the same as given by Proudman & Pearson (1957),

$$\mathrm{D}_\rho^2\,\Psi_{20} = \mathrm{e}^{\rho\mu/2} \sum_{n=1}^{\infty} A_n (\tfrac{1}{2}\rho)^{\frac{1}{2}} K_{n+\frac{1}{2}}(\tfrac{1}{2}\rho)\, Q_n(\mu), \tag{38}$$

where $k_{n+\frac{1}{2}}(\frac{1}{2}\rho)$ is the modified Bessel function. It can be expressed as

$$(\tfrac{1}{2}\rho)^{\frac{1}{2}} K_{n+\frac{1}{2}}(\tfrac{1}{2}\rho) = (\tfrac{1}{2}\pi)^{\frac{1}{2}} \mathrm{e}^{-\rho/2} \sum_{m=0}^{n} \frac{(n+m)!}{(n-m)!\,m!} \frac{1}{\rho^m}. \tag{39}$$

For small values of ρ, the least-singular term for $\mathrm{D}_\rho^2\,\Psi_{20}$ is of order $(1/\rho)\,Q_1(\mu)$ when $n = 1$. Expressing this least-singular part of $\mathrm{D}_\rho^2\,\Psi_{20}$ in terms of the inner variable and noting that $\mathrm{D}_\rho^2\,\Psi = \mathrm{D}_r^2\,\psi$, one has

$$\frac{St}{Re'}\mathrm{D}_\rho^2\,\Psi_{20} \sim \frac{St}{Re'}\frac{1}{Re'r} Q_1(\mu). \tag{40}$$

It is obvious that none of the terms in (39), including the above, can be matched to any of the inner solution with $\mathrm{D}_r^2\,\psi \sim O(St/Re'^2)$. This means that

$$\mathrm{D}_\rho^2\,\Psi_{20} = 0. \tag{41}$$

The boundary condition at infinity and the matching with the inner solution demand

$$\Psi_{20} = 0. \tag{42}$$

Substitution of $\Psi_{20} = 0$ into (29) yields the following equation for Ψ_{21}:

$$D_\rho^4 \Psi_{21} - \frac{(1-\mu^2)}{\rho}\frac{\partial D_\rho^2 \Psi_{21}}{\partial \mu} - \mu \frac{\partial D_\rho^2 \Psi_{21}}{\partial \rho} = \mathrm{i}\left[\frac{3}{2}\left(\frac{1}{\rho}+\frac{1}{2}\right)(1-\mu^2) - \tfrac{3}{8}\rho(1-\mu^2) - \tfrac{3}{4}(\rho+2)\,Q_2(\mu)\right]\mathrm{e}^{-\rho(1-\mu)/2}. \quad (43)$$

Equation (43) is similar to (28) except for the driving term on the right-hand side. The homogeneous solution for $D_\rho^2 \Psi_{21}$ is the same as given in (38). The particular solution to (43) can be found by applying Goldstein's transformation,

$$D_\rho^2 \Psi_{21} = \mathrm{e}^{\rho\mu/2}\Phi. \quad (44)$$

Equation (43) reduces to

$$(D_\rho^2 - \tfrac{1}{4})\Phi = -\mathrm{i}\left[\frac{3}{2}\left(\frac{1}{\rho}+\frac{1}{2}\right)(1-\mu^2) - \tfrac{3}{8}\rho(1-\mu^2) - \tfrac{3}{4}(\rho+2)\,Q_2(\mu)\right]\mathrm{e}^{-\rho/2}. \quad (45)$$

Assuming a particular solution for Φ in the form of

$$\Phi^{\mathrm{p}} = \mathrm{i}[g_1(\rho)(1-\mu^2) + g_2(\rho)\,Q_2(\mu)], \quad (46)$$

one obtains the following equations for $g_1(\rho)$ and $g_2(\rho)$:

$$g_1'' - \left(\frac{2}{\rho^2}+\frac{1}{4}\right)g_1 = \left[-\frac{3}{2}\left(\frac{1}{\rho}+\frac{1}{2}\right) + \tfrac{3}{8}\rho\right]\mathrm{e}^{-\rho/2}, \quad (47)$$

and

$$g_2'' - \left(\frac{6}{\rho^2}+\frac{1}{4}\right)g_2 = \tfrac{3}{4}(\rho+2)\,\mathrm{e}^{-\rho/2}. \quad (48)$$

Solving the ordinary differential equations for $g_1(\rho)$ and $g_2(\rho)$, the particular solution for Φ is

$$\Phi^{\mathrm{p}} = \mathrm{i}[\tfrac{3}{4}\rho(1-\mu^2) - \tfrac{3}{16}\rho^2(1-\mu^2) - \tfrac{3}{8}\rho^2 Q_2(\mu)]\,\mathrm{e}^{-\rho/2}, \quad (49)$$

which in turn gives the particular solution for $D_\rho^2 \Psi_{21}$ as

$$D_\rho^2 \Psi_{21}^{\mathrm{p}} = \mathrm{i}[\tfrac{3}{4}\rho(1-\mu^2) - \tfrac{3}{16}\rho^2(1-\mu^2) - \tfrac{3}{8}\rho^2 Q_2(\mu)]\,\mathrm{e}^{-\rho(1-\mu)/2}. \quad (50)$$

Letting

$$\Psi_{21}^{\mathrm{p}}(\rho,\mu) = \mathrm{i}F(\rho,\mu)\,\mathrm{e}^{-\rho/2(1-\mu)}, \quad (51)$$

equation (50) becomes

$$\frac{(1-\mu^2)}{\rho^2}\frac{\partial^2 F}{\partial \mu^2} + \frac{(1-\mu^2)}{\rho}\frac{\partial F}{\partial \mu} + \frac{\partial^2 F}{\partial \rho^2} - (1-\mu)\frac{\partial F}{\partial \rho} + \frac{1-\mu}{2}F = \tfrac{3}{4}\rho(1-\mu^2) - \tfrac{3}{16}\rho^2(1-\mu^2) - \tfrac{3}{8}\rho^2 Q_2(\mu). \quad (52)$$

A particular solution that satisfies (52) is

$$F(\rho,\mu) = -\tfrac{3}{8}\rho^2(1-\mu^2). \quad (53)$$

Therefore, the particular solution to (43) for Ψ_{21} is

$$\Psi_{21}^{\mathrm{p}}(\rho,\mu) = -\mathrm{i}\tfrac{3}{8}\rho^2(1-\mu^2)\,\mathrm{e}^{-\rho(1-\mu)/2}. \quad (54)$$

The general solution for Ψ_{21} is zero. It is determined by matching the outer solution Ψ with the inner solution ψ using arguments similar to those leading to (41) and (42) (see Mei 1990 for details). Thus

$$\Psi_{21} = \Psi_{21}^{\mathrm{p}}(\rho,\mu) = -\mathrm{i}\tfrac{3}{8}\rho^2(1-\mu^2)\,\mathrm{e}^{-\rho(1-\mu)/2}, \quad (55)$$

and
$$\psi_{20} = -\mathrm{i}\frac{3}{4}\left[\frac{1}{4}\left(2r^2-3r+\frac{1}{r}\right)(1-\mu^2)\right] \tag{56}$$

which satisfies (19) and matches Ψ_{21} to the leading order.

In summary, the flow field in the inner region is described by

$$\begin{aligned}
\psi(r,\mu) &\approx \psi_{\mathrm{s}}(r,\mu)+\alpha_1 \mathrm{e}^{-\mathrm{i}t}\psi_1(r,\mu)\\
&\approx \frac{1}{4}\left(2r^2-3r+\frac{1}{r}\right)(1-\mu^2)\\
&\quad +Re'\left[\frac{3}{32}\left(2r^2-3r+\frac{1}{r}\right)(1-\mu^2)+\frac{3}{16}\left(2r^2-3r+1-\frac{1}{r}+\frac{1}{r^2}\right)Q_2(\mu)\right]\\
&\quad +\alpha_1 \mathrm{e}^{\mathrm{i}t}\left\{\frac{1}{4}\left(2r^2-3r+\frac{1}{r}\right)(1-\mu^2)\right.\\
&\quad +Re'\left[\frac{3}{16}\left(2r^2-3r+\frac{1}{r}\right)(1-\mu^2)+\frac{3}{8}\left(2r^2-3r+1-\frac{1}{r}+\frac{1}{r^2}\right)Q_2(\mu)\right]\\
&\quad \left.+St(-\mathrm{i}\tfrac{3}{4})\left[\frac{1}{4}\left(2r^2-3r+\frac{1}{r}\right)\left(1-\mu^2\right)\right]\right\}.
\end{aligned} \tag{57}$$

The outer solution is described by

$$\begin{aligned}
\Psi(\rho,\mu) &\approx \Psi_{\mathrm{s}}(\rho,\mu)+\alpha_1 \mathrm{e}^{-\mathrm{i}t}\,\Psi_1(\rho,\mu)\\
&\approx \tfrac{1}{2}\rho^2(1-\mu^2)-Re'\tfrac{3}{2}Q_0(\mu)\{1-\exp[-\tfrac{1}{2}\rho(1-\mu)]\}\\
&\quad +\alpha_1 \mathrm{e}^{-\mathrm{i}t}\{\tfrac{1}{2}\rho^2(1-\mu^2)-Re'\tfrac{3}{4}\rho(1-\mu^2)\exp[-\tfrac{1}{2}\rho(1-\mu)]\\
&\quad +St(-\mathrm{i}\tfrac{3}{8})\rho^2(1-\mu^2)\mathrm{e}^{-\rho(1-\mu)/2}\}.
\end{aligned} \tag{58}$$

The drag on the sphere can now be evaluated from the inner solution given by (57). The contributions to the total drag are from the terms containing $(1-\mu^2)$ because $Q_2(\mu)$ is antisymmetrical. Note that the first term of ψ in (57) is the steady Stokes solution and the rest of the contributing terms have the same radial dependence $(2r^2+3r+1/r)$, so the drag coefficient is easily obtained as

$$\begin{aligned}
C_D/C_{D\mathrm{s}} &= 1+\tfrac{3}{8}Re'+\alpha_1 \mathrm{e}^{-\mathrm{i}t}\{1+\tfrac{3}{4}Re'+\ldots-\mathrm{i}\tfrac{3}{4}St+\ldots\}\\
&= D_{\mathrm{Steady}}+\alpha_1 \mathrm{e}^{-\mathrm{i}t}[D_{1\mathrm{R}}+\mathrm{i}D_{1\mathrm{I}}],
\end{aligned} \tag{59}$$

where $C_{D\mathrm{s}} = 24/Re = 12/Re'$ is the drag coefficient of the steady Stokes flow over a sphere. In (59), the leading-order unsteady drag is $D_{1\mathrm{R}} = 1+\frac{3}{4}Re'$. This is independent of the frequency and it is in fact the quasi-steady component of the unsteady drag. The real part of the acceleration-dependent drag was shown to be of $O(St^2)$ in MLA. The leading-order acceleration-dependent drag is $\mathrm{i}D_{1\mathrm{I}} = -\mathrm{i}\frac{3}{4}St$ which is linearly proportional to the frequency. The significance of (59) is that, through detailed analysis, the leading-order term of the acceleration-dependent unsteady drag at low frequency is again shown to be of $O(St)$, which agrees with the finding of MLA based on the finite-difference results. It shows that the Stokes solution for the unsteady problem is not valid at low frequency. The reason why the Stokes solution fails to describe the low-frequency drag may be explained as follows.

As pointed out in MLA, there are three lengthscales in this low-Reynolds-number, unsteady flow, $l_{\mathrm{Stokes}} \sim O(1)$ for the Stokes region where diffusion is dominant, $l_{\mathrm{Oseen}} \sim O(Re^{-1})$ for the Oseen region where convection is important, and

$l_{\text{unsteady}} \sim O(\epsilon^{-1})$ (see (63) for ϵ) for the region where unsteadiness is important. At low frequency, such that $l_{\text{Oseen}}/l_{\text{unsteady}} = \epsilon/Re \ll 1$, the vorticity generated on the wall decays exponentially in the Oseen region. Thus the region $r \sim l_{\text{unsteady}}$ is not dynamically important in transporting the vorticity. The present analysis takes this subtle, but important, point into consideration in formulating the asymptotic expansion. However, the Stokes solution, neglecting the convection mechanism of the vorticity transport, assumes that the region $r \sim l_{\text{unsteady}}$ is always important dynamically and that the unsteady term always balances the diffusion term. This is not true at low frequency. Thus, the dynamics of the vorticity transport surrounding the sphere are incorrectly described by the Stokes solution.

3. Comparison between the asymptotic analysis and the finite-difference solution

In order to assess the validity and accuracy of the above analytical results, the numerical results of MLA are next compared with them. The numerical results were obtained using the finite-difference method and they are valid for finite Re. The smallest Reynolds number computed was $Re = 0.1$, or $Re' = 0.05$. The smallest Strouhal number investigated at $Re' = 0.05$ was $St = 0.0025$. The result of the present asymptotic analysis, is valid only for $St/Re' \ll 1$ and $Re' \ll 1$. The parameters $(Re', St) = (0.05, 0.0025)$ can be considered to fall in the ranges of the validity of the asymptotic analysis, i.e. $St/Re' = 0.05 \ll 1$ and $Re' = 0.05 \ll 1$. Thus the comparison is meaningful.

The numerical solution for the unsteady stream function is represented as $\psi_1 = \psi_{1R} + i\psi_{1I}$. Figure 1 (*a*) compares the finite-difference solution of ψ_{1I}/St with the corresponding analytical solution based on the matched asymptotic expansion at $\theta = \frac{1}{2}\pi$ from $r = 1$ to $r = 150$. The inner and outer solutions of (57) and (58) are used to approximate the analytical solution, given as

$$-\psi_{1I}/St \sim \frac{3}{16}\left\{-3r + \frac{1}{r} + 2r^2 \exp\left[-\tfrac{1}{2}Re'\, r(1-\mu)\right]\right\}(1-\mu^2). \tag{60}$$

As $(r-1) \to 0$, (60) gives negative values near $r = 1$. Thus the inner solution in (57) is used for $r - 1 < 0.1$. The above expression is not valid for very large r because the $O(r)$ term in (60) is not matched between the inner and outer solutions. However, in the finite computational domain ($1 \leqslant r \leqslant 150$), the comparison between the finite-difference solution and the analytical solution is surprisingly good. The discrepancy in the inner region is of $O(Re')$, and it results because the solution to (20) for ψ_{21} is not pursued.

Figure 1 (*b*) compares the real component of the unsteady stream function, $\psi_{1R}(r, \theta = \frac{1}{2}\pi)$, of the finite-difference solution and of the asymptotic solution at $(Re', St) = (0.05, 0.0025)$. This corresponds to the quasi-steady-state solution. The agreement is very good for ψ_{1R} varying from 0.00346 at the first grid away from the wall to 10901 at $r \approx 150$. The difference near the wall is again of $O(Re')$ and it is due to the neglect of the higher-order terms in the analytical solution.

In the region close to the wall, both real and imaginary parts of the analytical solution for the stream function have errors of $O(Re')$ compared with the finite-difference solution. However, the vorticity, $(1/r\sin\theta)\,\mathrm{D}_r^2\psi$, of the two solutions agrees very well on the wall. Figure 2 compares the imaginary part of the analytical wall vorticity at $(Re', St) = (0.05, 0.0025)$ with the numerical solution. The slight asymmetry of the numerical solution with respect to $\theta = \frac{1}{2}\pi$ is due to the small

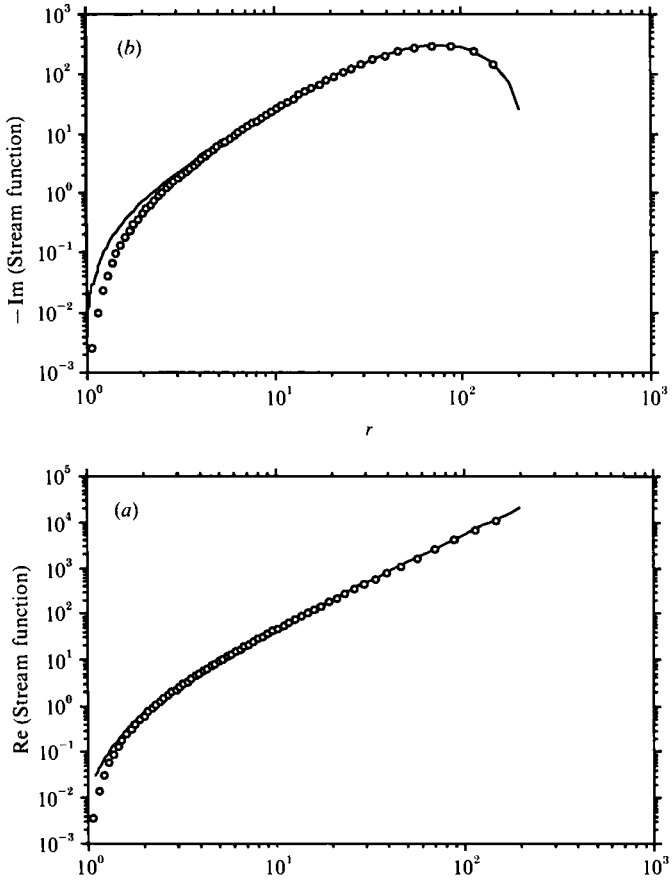

FIGURE 1. Comparison between the stream functions of the asymptotic (——) and the finite-difference (○) solutions at $Re' = 0.05$, $St = 0.0025$ and $\theta = \frac{1}{2}\pi$ from $r = 1$ to 150. (*a*) Imaginary or acceleration-dependent part, (*b*) real or quasi-steady part at low St.

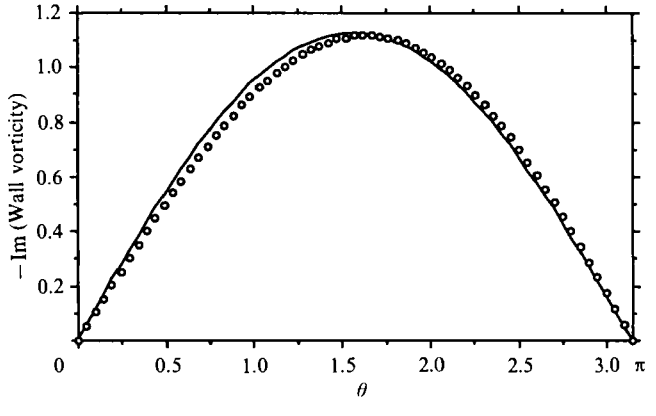

FIGURE 2. Comparison between the imaginary part of the unsteady wall vorticity of the asymptotic (——) and finite-difference (○) solutions at $(Re', St) = (0.05, 0.0025)$.

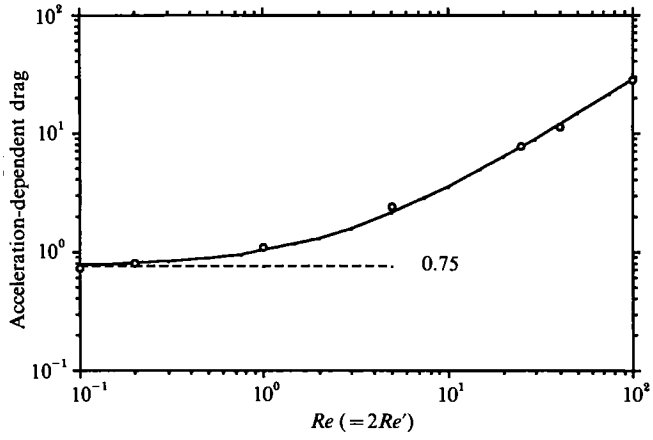

FIGURE 3. Dependence of the acceleration-dependent part of the unsteady drag on Re at very small St: ○, finite difference; ——, $f(Re) = 0.75 + 0.272Re$; – – – –, matched asymptotic expansion.

nonlinearity picked up in the computation. This asymmetry may be associated with $Q_2(\mu)$, and it has a high-order effect which does not appear in the lower-order asymptotic expansion.

Figure 3 shows $f(Re') = \lim_{St\to 0}(D_{1I}/St)$, the acceleration-dependent drag scaled by St, as a function of Re at very small frequency, for Re ranging from 0.1 to 100. The numerical values of $f(Re')$ are obtained by taking D_{1I}/St from the smallest St computed for each Re. The smallest St for each computation is chosen such that, as the frequency doubles, the new D_{1I} increases by a factor of two. It can be seen that the numerical solution approaches the analytical prediction of $D_{1I}/St = 0.75$ as $Re \to 0$. The accuracy of the low-Reynolds-number asymptotic solution in predicting the unsteady drag is confirmed. For finite Re', a curve-fit based on the analytical and numerical results can be obtained to approximate $f(Re')$:

$$D_{1I}(St) \approx -f(Re')\,St = -(0.75 + 0.544Re')\,St. \tag{61}$$

The corresponding imaginary part of the history force, D_{1IH}, at low frequency is

$$\begin{aligned} D_{1IH}(St) &= D_{1I}(St) - \mathrm{Im}\,(D_{\text{added-mass}}(\epsilon) + D_{\text{accel. frame}}(\epsilon)) \\ &= -f(Re')\,St - \tfrac{2}{3}\epsilon^2 \\ &= -f_H(Re')\,St = -(0.75 + 0.211Re')\,St \end{aligned} \tag{62}$$

(see (64*b*) for $D_{\text{added-mass}}$ and $D_{\text{accl. frame}}$) where

$$\epsilon = (Re\,St/4)^{\frac{1}{2}} = (\tfrac{1}{2}Re'\,St)^{\frac{1}{2}} \tag{63}$$

is the Stokes number. It should be noted that the results of the numerical solution are based on $Re \leqslant 100$. Thus, (62) may be valid only for $Re' \leqslant 50$. Equation (62) will be used next to derive a general expression for $D_{1IH}(St)$ at finite frequency.

4. Behaviour of the unsteady drag in the time domain at finite Reynolds number

In this section, equation (62), the Stokes solution at high frequency, and the numerical results of MLA are used to obtain and verify a general expression for $D_{1IH}(St)$ in the frequency domain. The principle of causality is then used to deduce the behaviour of the history force in the time domain.

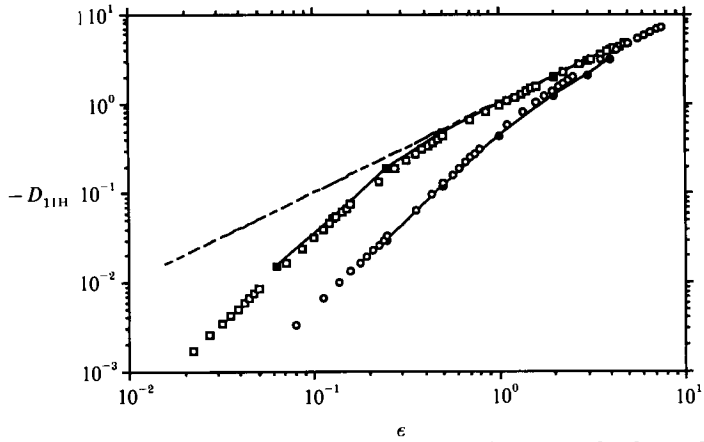

FIGURE 4. Comparison between the imaginary part of the unsteady drag of the finite-difference solution (filled symbols) and the direct interpolation (open symbols) at $Re' = 0.5$ (□) and $Re' = 12.5$ (○). Dashed line is Stokes solution.

For the problem considered here, the unsteady component of the drag of the Stokes solution in the frequency domain has the form

$$\tilde{D}_1(\omega) = 1 + (1-\mathrm{i})\,\epsilon - \mathrm{i}\tfrac{2}{9}\epsilon^2 - \mathrm{i}\tfrac{4}{9}\epsilon^2. \tag{64a}$$

Correspondingly, the unsteady drag at *finite Reynolds number* can be represented as

$$\tilde{D}_1(\omega) = D_{\mathrm{QS}}(Re) + D_{1\mathrm{H}}(Re', St) + D_{\text{added-mass}}(\epsilon) + D_{\text{accel. frame}}(\epsilon) \tag{64b}$$

(see MLA for details). The term $(1-\mathrm{i})\,\epsilon$ in (64a) corresponds to the Basset force. For finite Reynolds number, the Stokes' solution (64a) remains valid asymptotically at high frequency, i.e. $\epsilon \gg 1$, because the Stokes layer of thickness $O(\epsilon^{-1})$ is the dominant structure in the immediate neighbourhood of the sphere. As shown in MLA, the smaller the Reynolds number, the closer the Stokes solution approaches the finite-difference solution. The term $D_{\text{accel. frame}}(\epsilon)$ is due to the acceleration of the reference frame that is attached to the sphere. If the free-stream velocity is steady and the sphere is oscillating, this term is zero.

For the intermediate range of values of St, an interpolation based on (62) and (64a) is proposed for the imaginary part of the history force

$$D_{1\mathrm{IH}}(St) \approx \frac{-f_{\mathrm{H}}(Re')\,St}{[1+(2f_{\mathrm{H}}^2(Re')\,St/Re')]^{\frac{1}{2}}}. \tag{65}$$

This expression recovers both (62) and (64a) when St is small or large. For intermediate St and for $Re' = 0.5$ and $Re' = 12.5$, the expression for $D_{1\mathrm{IH}}(St)$ given above is compared with the numerically computed value of $D_{1\mathrm{IH}}(St)$ in figure 4. Equation (65) is confirmed by the finite-difference results.

A similar interpolation could be devised for $D_{1\mathrm{RH}}(St)$. However, knowing either $D_{1\mathrm{IH}}(St)$ or $D_{1\mathrm{RH}}(St)$ is sufficient to deduce the history force in the time domain. This statement will be justified later.

Consider α_1 as a function of ω and treat $\tilde{u}_1'(\omega) = \alpha_1(\omega)\,U$ as the Fourier component of $u_1'(t')$, i.e.

$$\tilde{u}_1'(\omega) = \alpha_1(\omega)\,U = \int_{-\infty}^{\infty} u_1'(t')\,\mathrm{e}^{\mathrm{i}\omega t'}\,\mathrm{d}t'. \tag{66}$$

The *dimensional* unsteady fluctuating velocity may be superimposed on the steady mean velocity U so that the unsteady part of the drag, $F'_1(t')$, corresponding to the unsteady velocity $u'_1(t')$ is

$$F'_1(t') = \frac{1}{2\pi}\int_{-\infty}^{\infty} \tilde{F}'_1(\omega)\, e^{-i\omega t'}\, d\omega, \tag{67}$$

with

$$\tilde{F}'_1(\omega) = 6\pi\mu a \tilde{u}'_1(\omega)\,[D_{QS}(Re') + D_{1H}(St, Re')] + D_{\text{added-mass}} + D_{\text{accel. frame}}. \tag{68}$$

Substitution of (68) into (67) yields

$$F'_1(t') = 6\pi\mu a D_{QS}(Re')\, u'_1(t') + 6\pi\mu a \frac{1}{2\pi}\int_{-\infty}^{\infty} D_{1H}(St, Re')\, \tilde{u}'_1(\omega)\, e^{-i\omega t'}\, d\omega + (\tfrac{1}{2}+1)\tfrac{4}{3}\pi a^3 \rho_f \frac{du'_1}{dt'}. \tag{69}$$

The first term in (69) is the quasi-steady drag; it is given as

$$D_{QS} = 1 + b(1+n)\, Re^n \tag{70}$$

in MLA, where $b = 0.15$ and $n = 0.687$ are the empirical constants (see Clift, Grace & Weber 1978). The combination of the steady-state drag and this quasi-steady drag may be expressed in one term as $6\pi\mu a D_S(Re(t))\,[U + u'_1(t')]$ with

$$D_S(Re(t)) = 1 + b[(U + u'_1(t'))\, 2a/\nu]^n.$$

The last term in (69) corresponds to the force due to the added mass and the free-stream acceleration. Numerical results show that the added-mass force is independent of the Reynolds number. The second term in (69) is the history force, $F'_H(t')$. It is a function of both Re and St. Using (67), the history force can be written as

$$\begin{aligned}\frac{F'_H(t')}{6\pi\mu a} &= \frac{1}{2\pi}\int_{-\infty}^{\infty} \frac{D_{1H}(\omega)}{-i\omega}\,[-i\omega\tilde{u}'_1(\omega)]\, e^{-i\omega t'}\, d\omega \\ &= \frac{1}{2\pi}\int_{-\infty}^{\infty} \frac{D_{1H}(\omega)}{-i\omega}\left[\int_{-\infty}^{\infty} \frac{du'_1}{d\tau} e^{i\omega\tau}\, d\tau\right] e^{-i\omega t'}\, d\omega \\ &= \int_{-\infty}^{\infty} K(t'-\tau)\frac{du'_1}{d\tau}\, d\tau, \end{aligned} \tag{71}$$

where

$$K(t'-\tau) = \frac{1}{2\pi}\int_{-\infty}^{\infty} \frac{D_{1H}(\omega)}{-i\omega} e^{-i\omega(t'-\tau)}\, d\omega \tag{72}$$

is the integration kernel of the history force. In the Stokes regime, the kernel is

$$K(t'-\tau) = \frac{H(t'-\tau)}{(\pi\nu(t'-\tau)/a^2)^{\frac{1}{2}}}$$

where $H(t'-\tau)$ is the Heaviside step function. For the present finite-Reynolds-number case, $K(t'-\tau)$ is expected to be proportional to the Heaviside step function based on the *principle of causality*, i.e. the motion of the particle can be influenced

only by its previous history, not by its future behaviour. This step-function behaviour of the history force kernel gives a condition to relate $D_{1\mathrm{RH}}(St)$ and $D_{1\mathrm{IH}}(St)$. For $\xi' = \tau - t' > 0$, (72) can be written as

$$K(-\xi') = \frac{1}{2\pi}\int_{-\infty}^{\infty} \frac{D_{1\mathrm{RH}}(\omega) + \mathrm{i}D_{1\mathrm{IH}}(\omega)}{-\mathrm{i}\omega}[\cos(\omega\xi') + \mathrm{i}\sin(\omega\xi')]\,\mathrm{d}\omega$$

$$= \frac{1}{2\pi}\int_{-\infty}^{\infty} -\frac{1}{\omega}[D_{1\mathrm{RH}}(\omega)\sin(\omega\xi') + D_{1\mathrm{IH}}(\omega)\cos(\omega\xi')]\,\mathrm{d}\omega$$

$$+\frac{\mathrm{i}}{2\pi}\int_{-\infty}^{\infty} -\frac{1}{\omega}[D_{1\mathrm{RH}}(\omega)\cos(\omega\xi') - D_{1\mathrm{IH}}(\omega)\sin(\omega\xi')]\,\mathrm{d}\omega = 0. \tag{73}$$

The imaginary part of (73) is zero because

$$D_{1\mathrm{RH}}(-\omega) = D_{1\mathrm{RH}}(\omega), \quad D_{1\mathrm{IH}}(-\omega) = -D_{1\mathrm{IH}}(\omega). \tag{74}$$

For the real part of $K(-\xi')$ to vanish, the following must hold for all values of $\xi' > 0$:

$$\int_0^{\infty} D_{1\mathrm{RH}}(\omega)\sin(\omega\xi')/\omega\,\mathrm{d}\omega = \int_0^{\infty} D_{1\mathrm{IH}}(\omega)\cos(\omega\xi')/\omega\,\mathrm{d}\omega. \tag{75}$$

Thus, $D_{1\mathrm{RH}}(\omega)$ can be evaluated from (75) once $D_{1\mathrm{IH}}(\omega)$ is given.

Now consider $\eta' = t' - \tau > 0$. The history force kernel can be written as

$$K(\eta') = \frac{-2}{2\pi}\int_{-\infty}^{\infty} \frac{1}{\omega} D_{1\mathrm{IH}}(\omega)\cos(\omega\eta')\,\mathrm{d}\omega,$$

i.e.
$$K(\eta) = \frac{2}{\pi}\int_0^{\infty} \frac{f_{\mathrm{H}}(Re')}{[1 + (2f_{\mathrm{H}}^2(Re')\,St/Re')]^{\frac{1}{2}}}\cos(St\,\eta)\,\mathrm{d}St, \tag{76}$$

where $\eta = \eta' U/a$ is the dimensionless time scaled by the free-stream mean velocity and the radius of the particle. A closed-form expression for the above integration can be obtained in terms of the Fresnel integral, but this expression is too complex to extract any useful information. Instead, we utilize the asymptotic behaviour of the $K(\eta)$. For small and large values of η, the following asymptotic expression can be obtained using the integration by parts for $K(\eta)$:

$$K(\eta) \sim \left(\frac{Re'}{\pi\eta}\right)^{\frac{1}{2}} \quad \text{for} \quad \eta \to 0 \tag{77}$$

and
$$K(\eta) \sim \frac{2f_{\mathrm{H}}^3(Re')}{\pi}\frac{1}{Re'}\frac{1}{\eta^2}, \quad \text{for} \quad \eta \to \infty. \tag{78}$$

Combining the above two expressions for $K(\eta)$, an interpolation is proposed for arbitrary η as follows:

$$K(\eta) \approx \left\{\left(\frac{\pi\eta}{Re'}\right)^{\frac{1}{4}} + \left[\tfrac{1}{2}\pi\frac{Re'}{f_{\mathrm{H}}^3(Re')}\eta^2\right]^{\frac{1}{2}}\right\}^{-2}. \tag{79}$$

To confirm the validity of the interpolation given by (79), a Fourier transform has been performed on the above $K(\eta)$ to obtain approximate values of $D_{1\mathrm{RH}}(St)$ and $D_{1\mathrm{IH}}(St)$ in the frequency domain. They are then compared with the corresponding finite-difference results. Figure 5 shows comparisons of $D_{1\mathrm{IH}}(St, Re' = 0.05)$,

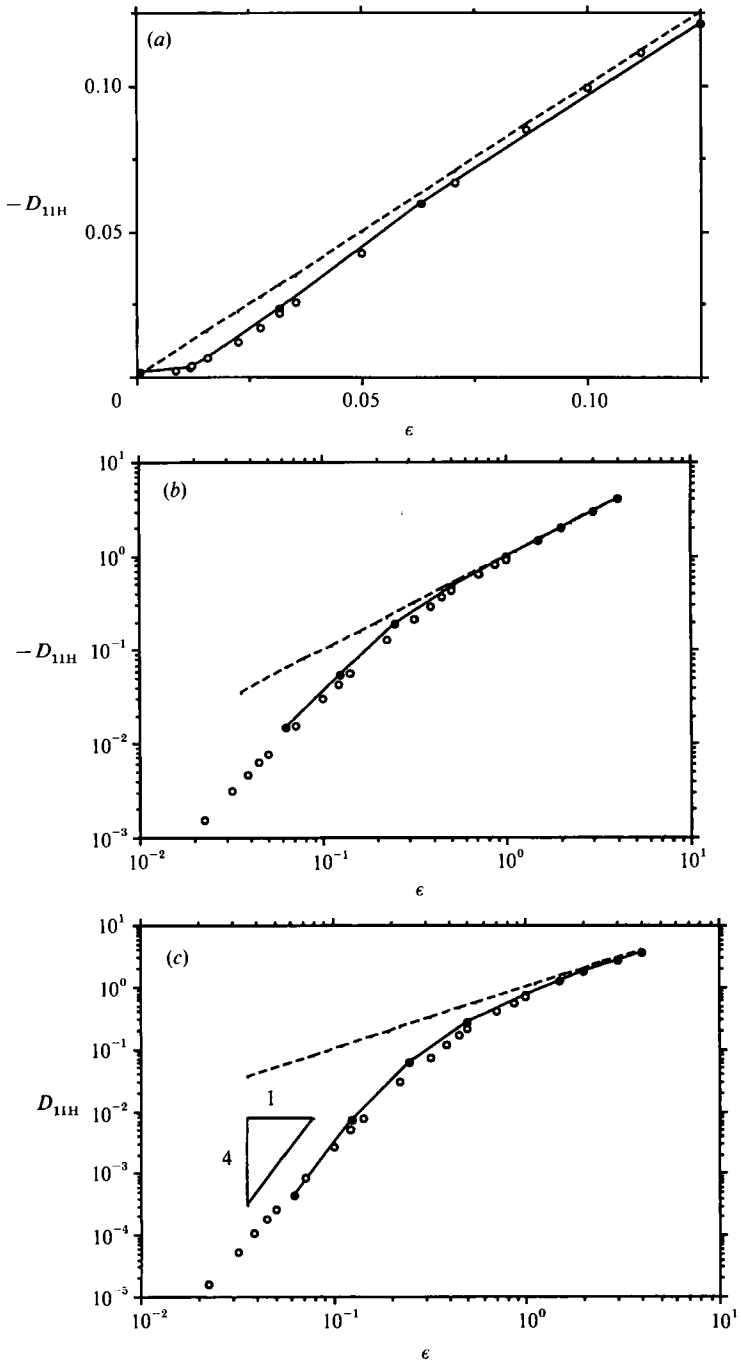

FIGURE 5. Comparison between the history force in the frequency domain, $D_{1H}(St)$, of the finite-difference solution (—●—) and that based on the Fourier transformation of the interpolated history force kernel $K(t'-\tau)$, equation (79) (○). (*a*) $-D_{11H}(St, Re' = 0.05)$; (*b*) $-D_{11H}(St, Re' = 0.5)$; (*c*) $D_{1RH}(St, Re' = 0.5)$. Dashed line is the Stokes solution.

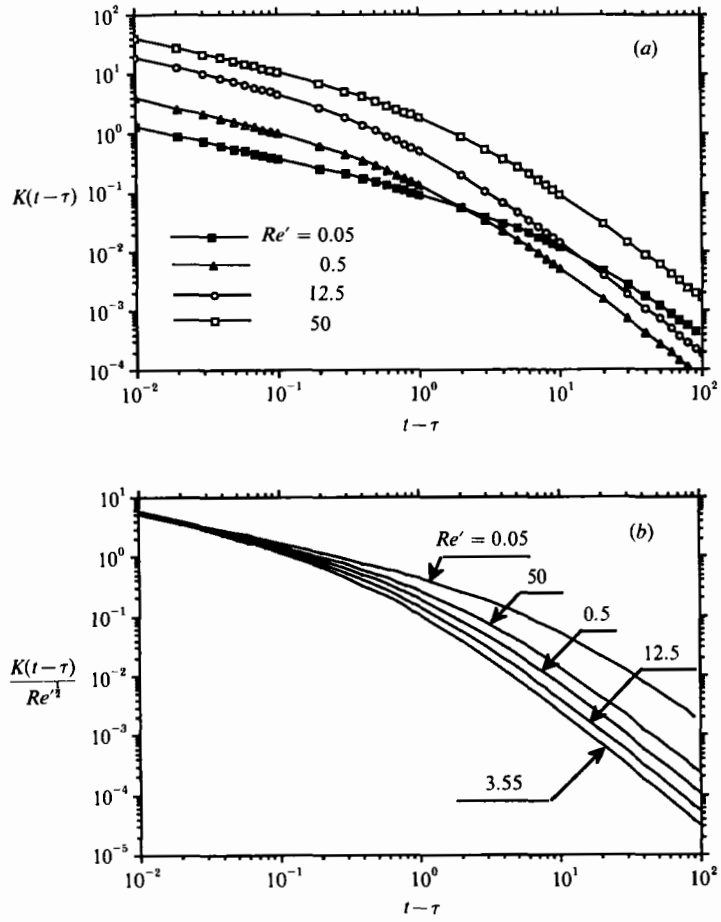

FIGURE 6. Behaviour of the modified history force kernel at various Reynolds numbers. (*a*) $K(t-\tau)$; (*b*) renormalized kernel $K(t-\tau)/Re'^{\frac{1}{2}}$.

$D_{1IH}(St, Re' = 0.5)$ and $D_{1RH}(St, Re' = 0.5)$ between the two types of $D_{1H}(St)$. They agree with each other very well over a wide range of Stokes numbers.

To recapitulate, the dimensional form of the modified history force in the time domain is given by

$$F'_H(t') = 6\pi\mu a \int_{-\infty}^{t'} K(t'-\tau)\frac{du'_1}{d\tau}d\tau, \tag{80}$$

where

$$K(t'-\tau) \approx \left\{\left[\frac{\pi(t'-\tau)\nu}{a^2}\right]^{\frac{1}{4}} + \left[\tfrac{1}{2}\pi\frac{U^3}{a\nu f_H^3(Re')}(t'-\tau)^2\right]^{\frac{1}{3}}\right\}^{-2}. \tag{81}$$

This expression for the history force is valid for particles possessing large slip velocity relative to the turbulence of the carrier fluid.

It is possible to generalize (80) and (81) to extend the application of the present modified history force to the more general situation regarding the particle motion in turbulence. The first is to change the lower integration limit from $-\infty$ to t'_0, where t'_0 is the instant when the particle is introduced to the fluid. This modification is exact because $du'_1/d\tau = 0$ for $t' < t'_0$. The second generalization is to replace U, the strong mean velocity, by $(\boldsymbol{u}-\boldsymbol{v})$, the instantaneous relative velocity between the fluid and

the particle. It is not entirely accurate and cannot be verified directly in the context of this study. The physical reason for this generalization is similar to that for approximating the quasi-steady drag using the steady-state drag coefficient and the instantaneous velocity difference. Here, we hypothesize that it is the form of the kernel that is most important dynamically and that the convection velocity, which defines $U(t)$ and $Re(t)$ in (81), only influences the results parametrically rather than dynamically.

Having obtained the history force kernel at finite Reynolds number, it is interesting to examine how the kernel is influenced by the Reynolds number, or the nonlinearity of the system. Figure 6(*a*) shows $K(t-\tau)$, given by (79), as a function of $(t-\tau)$ at $Re' = 0.05$, 0.5, 12.5 and 50. At small $(t-\tau)$, the kernel behaves as $(t-\tau)^{-\frac{1}{2}}$ and increases with Re'. At large $(t-\tau)$, it decreases in time as $(t-\tau)^{-2}$ but has a more complex dependence on the Reynolds number: $K(t-\tau, Re' = 0.05)$ is larger than K for $Re' = 0.5$ and K for $Re' = 12.5$, but it is less than that for $Re' = 50$. To see the effect of Reynolds number more clearly, the kernel is renormalized by $Re'^{\frac{1}{2}}$ and the dependence of $K(t-\tau, Re')/Re'^{\frac{1}{2}}$ on $(t-\tau)$ and Re' is shown in figure 6(*b*). At small times, say $(t-\tau) < 0.1$, the renormalized kernel is almost independent of Re', and the Basset (1888) solution is certainly a good approximation for small time. At larger $(t-\tau), K(t-\tau, Re')/Re'^{\frac{1}{2}}$ decreases as Re' increases for $0 < Re' < Re'^*$ with $Re'^* \approx 0.75/0.211 = 3.55$. This Re'^* is obtained by taking the derivative of $Re'^{\frac{3}{2}}/(0.75+0.211Re')^3$ with respect to Re' and setting it zero. At $Re' > Re'^*$, the renormalized kernel increases with Re'. This is probably due to the nonlinear interaction between the boundary layer of the steady flow (as Reynolds number increases) and the oscillating free stream. The present result for $K(t-\tau, Re')$ clearly shows that the classical Basset history force is not uniformly valid for long time even for very small Reynolds number, which one might consider as a Stokes flow problem.

5. Discussion of the unsteady drag formula by Odar & Hamilton

Odar & Hamilton (1964) performed an experiment to investigate the unsteady drag of a sphere executing a sinusoidal oscillation in an oil tank. They proposed a formula for the unsteady drag at finite Reynolds number based on their experimental results. It consists of the quasi-steady-state drag (which is independent of the acceleration), the modified history force, and the modified added-mass force,

$$F = \tfrac{1}{2}\rho_f \pi a^2 C_D(t)\,|U(t)|\,U(t) + C_H\, a^2(\pi\mu\rho_f)^{\frac{1}{2}} \int_{-\infty}^{t'} \frac{\mathrm{d}U}{\mathrm{d}\tau}\frac{\mathrm{d}\tau}{[\pi\nu(t'-\tau)]^{\frac{1}{2}}} + C_A\,\tfrac{4}{3}\rho_f \pi a^3 \frac{\mathrm{d}U}{\mathrm{d}t}, \tag{82}$$

where C_D is the steady-state drag coefficient evaluated with the instantaneous Reynolds number, and C_H and C_A are the modifying coefficients for the history force and the added-mass force. The modification is mainly governed by an 'acceleration' parameter,

$$A_c = \frac{U^2(t)}{2a|\mathrm{d}U/\mathrm{d}t|}, \tag{83}$$

i.e. the ratio of instantaneous velocity to the acceleration of the oscillating sphere. The modifying coefficients are given as (see Odar 1966)

$$C_H = 2.88 + 3.12/(A_c+1)^3; \quad C_A = 1.05 - 0.066/(A_c^2+0.12). \tag{84}$$

Their formula seems to agree well with their experimental data. However, there are two specific aspects that should be addressed here.

First, in their formulation, it was assumed *a priori* that the history force in the time domain is still proportional to

$$\int_{-\infty}^{t'} \frac{\mathrm{d}U}{\mathrm{d}\tau} \frac{\mathrm{d}\tau}{[\pi\nu(t'-\tau)]^{\frac{1}{2}}}.$$

The latter may be valid only at zero Reynolds number, in view of the foregoing analyses and discussion. There is apparently little justification for expressing the history force at finite Reynolds number in the form (82) without considering the possible changes in the integration kernel which result from the nonlinearity of the system, as the present study has indicated. Modification by introducing the coefficient C_{H} in front of the integration is neither physically justified nor mathematically rigorous.

Secondly, it should be noted that the Basset solution for unsteady drag in the time domain in the Stokes flow regime is derivable from the Fourier transformation of the unsteady drag in the frequency domain (see Landau & Lifshitz 1959). The data for the unsteady drag in the frequency domain must cover a large range of frequencies. In Odar & Hamilton's (1964) experiment, only a few discrete frequencies were investigated, and the frequencies were actually quite large in terms of the Stokes number. From the standpoint of Fourier transformation, it is not possible to infer the behaviour of the unsteady drag in the time domain from a small number of data points in the frequency domain, whether the time period in measuring the unsteady force for single harmonic oscillation is small or large. The fact that the total unsteady drag based on their expressions for the history force and the added-mass force agrees very well with their measured value suggests that the errors in the history force and in the added-mass force merely cancel each other owing to the way they were constructed. Unphysical features associated with their expressions for the modified history force and the added-mass force on a sphere executing a single harmonic oscillation in a stagnant liquid have been uncovered (Mei 1991) near the instant when $U(t) = 0$ for low and moderate frequencies, and they indeed cancel each other in the expression for the total unsteady drag on an oscillating sphere. They may not, however, always cancel in other kinds of unsteady flows.

6. Conclusions

A matched asymptotic solution for the unsteady Navier–Stokes equation has been obtained for axisymmetric flow over a stationary sphere at small Reynolds number with small, low-frequency fluctuations in the free-stream velocity. The unsteady drag due to the small-amplitude oscillation in the stream velocity is examined and compared with that obtained using the finite-difference method. At small Reynolds number, the acceleration-dependent force computed is lincarly proportional to the frequency. The classical Stokes solution is not valid at small ω for small values of Reynolds numbers.

The behaviour of the history force in the time domain has been examined based on the analytical results for small Re and the numerical results at finite Re. An expression is proposed to modify the history force for small and finite Reynolds numbers. The integration kernel decays as $(t'-\tau)^{-2}$ at large time, rather than the classical behaviour of $(t'-\tau)^{-\frac{1}{2}}$, even for very small Reynolds numbers. The expression for the modified history force in the time domain is verified by Fourier transforming the interpolated expression in the time domain into the frequency domain and comparing it with the finite-difference results which are obtained in the frequency

domain. Present results are valid for the case of small-amplitude fluctuations in the free-stream velocity but may be generalized to cases with large-amplitude fluctuations.

The authors wish to thank Professor Christopher J. Lawrence for his comments. This paper is based on the Ph.D thesis of the first author. This work was partially supported by the Department of Energy through Argonne National Laboratory Contract 82862403.

REFERENCES

ACKERBERG, R. C. & PHILLIPS, J. H. 1972 The unsteady laminar boundary layer on a semi-infinite flat plate due to small fluctuations in the magnitude of the free-stream velocity. *J. Fluid Mech.* **51**, 137–157.

BASSET, A. B. 1888 *A Treatise on Hydrodynamics*, vol. 2. Dover.

CLIFT, R., GRACE, J. R. & WEBER, M. E. 1978 *Bubbles, Drops and Particle.* Academic.

LANDAU, L. E. & LIFSHITZ, E. M. 1959 *Fluid Mechanics.* Pergamon.

LIGHTHILL, M. J. 1954 The response of laminar skin friction and heat transfer to fluctuations in the stream velocity. *Proc. R. Soc. Lond.* A **224**, 1–23.

MEI, R. 1990 Particle dispersion in isotropic turbulence and unsteady particle dynamics at finite Reynolds number. Ph.D thesis, University of Illinois at Urbana-Champaign.

MEI, R. 1991 Flow due to an oscillating sphere and an expression for unsteady drag on the sphere at finite Reynolds number. *Rep.* AeMES TR-91-2-01. Department of Aero. Engng, Mech. & Engng Sci., University of Florida.

MEI, R., LAWRENCE, C. J. & ADRIAN, R. J. 1991 Unsteady drag on a sphere at finite Reynolds number with small fluctuations in the free-stream velocity. *J. Fluid Mech.* **233**, 613–631 (referred to herein as MLA).

MEI, R. & PLOTKIN, A. 1986 A finite difference scheme for the solution of the steady Navier–Stokes equation. *Comput. Fluids* **14**, 239–251.

ODAR, F. 1966 Verification of the proposed equation for calculation of the forces on a sphere accelerating in a viscous fluid. *J. Fluid Mech.* **25**, 591–592.

ODAR, F. & HAMILTON, W. S. 1964 Forces on a sphere accelerating in a viscous fluid. *J. Fluid Mech.* **18**, 302–314.

PROUDMAN, I. & PEARSON, J. R. A. 1957 Expansions at small Reynolds numbers for the flow past a sphere and a circular cylinder. *J. Fluid Mech.* **2**, 237–262.

STOKES, G. G. 1851 On the effect of internal friction of fluids on the motion of pendulum. *Trans. Camb. Phil. Soc.* **9**, 8. (Reprinted in *Mathematical and Physical Papers*, vol. III. Cambridge University Press, 1922).